Published in final edited form as:
Cancer Discov. 2013 October ; 3(10): . doi:10.1158/2159-8290.CD-13-0118.

Hypoxia-Dependent Modification of Collagen Networks Promotes Sarcoma Metastasis

T.S. Karin Eisinger-Mathason[1,2], **Minsi Zhang**[3], **Qiong Qiu**[4], **Nicolas Skuli**[1,2,5], **Michael S. Nakazawa**[1,2], **Tatiana Karakasheva**[1,2], **Vera Mucaj**[1,2], **Jessica E.S. Shay**[1,2], **Lars Stangenberg**[6], **Navid Sadri**[2], **Ellen Puré**[7], **Sam S. Yoon**[8], **David G. Kirsch**[3,4], and **M. Celeste Simon**[1,2,5]

[1]Abramson Family Cancer Research Institute, University of Pennsylvania, Philadelphia, PA 19104, USA

[2]Perelman School of Medicine, University of Pennsylvania, Philadelphia, PA 19104, USA

[3]Department of Pharmacology and Cancer Biology, Duke University Medical Center, Durham NC 27708, USA

[4]Department of Radiation Oncology, Duke University Medical Center, Durham NC 27708, USA

[5]Howard Hughes Medical Institute, Massachusetts General Hospital, Boston, MA 02114, USA

[6]Department of Surgery, Massachusetts General Hospital, Boston, MA 02114, USA

[7]The Wistar Institute, Philadelphia, PA 19104

[8]Memorial Sloan Kettering Cancer Center, New York, NY 10065

Abstract

Intratumoral hypoxia and expression of Hypoxia Inducible Factor 1α (HIF1α) correlate with metastasis and poor survival in sarcoma patients. We demonstrate here that hypoxia controls sarcoma metastasis through a novel mechanism wherein HIF1α enhances expression of the intracellular enzyme procollagen-lysine, 2-oxoglutarate 5-dioxygenase 2 (PLOD2). We show that loss of HIF1α or PLOD2 expression disrupts collagen modification, cell migration and pulmonary metastasis (but not primary tumor growth) in allograft and autochthonous *LSLKras*$^{G12D/+}$; *Trp53*$^{fl/fl}$ murine sarcoma models. Furthermore, ectopic PLOD2 expression restores migration and metastatic potential in HIF1α-deficient tumors, and analysis of human sarcomas reveal elevated *HIF1α* and *PLOD2* expression in metastatic primary lesions. Pharmacological inhibition of PLOD enzymatic activity suppresses metastases. Collectively, these data indicate that HIF1α controls sarcoma metastasis through PLOD2-dependent collagen modification and organization in primary tumors. We conclude that PLOD2 is a novel therapeutic target in sarcomas and successful inhibition of this enzyme may reduce tumor cell dissemination.

Keywords

metastasis; sarcoma; HI1α; PLOD2; collagen; hypoxia

Corresponding author: M. Celeste Simon, PhD Scientific Director and Investigator, Abramson Family Cancer Research Institute Investigator, Howard Hughes Medical Institute Professor, Cell and Developmental Biology University of Pennsylvania, Perelman School of Medicine 456 BRB II/III, 421 Curie Boulevard Philadelphia, PA 19104-6160 Telephone number: 215-746-5532 Fax number: 215-746-5511 celeste2@mail.med.upenn.edu.

Conflict of interest: The authors declare no competing financial interests

Introduction

Sarcomas are diagnosed in 200,000 people worldwide annually; approximately 40% of whom ultimately succumb to lethal metastases (1, 2). Current treatment options available to sarcoma patients are standard surgical resection, radiation, and chemotherapy, and limited molecular analyses of human sarcomas have proven an impediment to developing novel, sarcoma-specific, therapeutic options. Although genetic lesions affecting multiple signaling pathways (*Kras, Pten, Ptch1, p53*) have been identified in distinct soft tissue sarcoma subtypes (3, 4), relatively little is understood about the downstream molecular mechanisms that drive sarcomagenesis and progression. Furthermore, soft tissue sarcomas encompass more than 50 distinct disease subtypes (e.g. fibrosarcoma, liposarcoma, rhabdomyosarcoma, etc.), all of which undergo constant reevaluation as developing technologies allow for more thorough characterization of each malignancy (5). As in other tumors, aggressive metastatic behavior in sarcomas is frequently associated with high levels of tumor cell dedifferentiation (6). Consistent with this observation, Undifferentiated Pleomorphic Sarcoma (UPS) has been identified as one of the most frequently diagnosed subtypes, and commonly results in lethal pulmonary metastases. Current data suggest that UPS may not represent a distinct sarcoma subtype, but rather a collection of phenotypes common to other sarcomas in their more advanced stages (7). It has been argued that UPS exists along a continuum wherein unique sarcoma subtypes become increasingly undifferentiated as they worsen in stage and grade until their tissue/cell type of origin is no longer discernible (7). Regardless of whether UPS is ultimately shown to be distinct or a culmination of sarcoma progression, these tumors are associated with poor clinical outcome due to metastases. As metastasis, particularly to the lungs, remains the most common cause of sarcoma-associated death, elucidating the molecular and cellular mechanisms controlling sarcoma cell dissemination is critical to the development of effective therapeutic strategies to treat these cancers.

The development of successful therapeutic interventions for sarcoma will depend on the ability to accurately model UPS and other subtypes. One mouse model for investigating UPS employs simultaneous Cre-dependent expression of oncogenic $Kras^{G12D}$ and deletion of p53 in the left gastrocnemius muscle (8). These genetic changes occur frequently in sarcoma and the murine tumors that develop recapitulate human UPS morphologically, histologically, and genetically (8, 9). Most importantly, primary tumors that develop in this autochthonous model successfully metastasize to the lung, mirroring human UPS. Furthermore, subcutaneous allografts of murine UPS cells will also metastasize to the lung within several weeks of implantation. Combined, these approaches allow for the investigation of molecular mechanisms that govern primary UPS formation and pulmonary metastases.

The available clinical data indicate that high levels of intratumoral hypoxia and HIF1α expression are among the most important predictors of metastatic potential in sarcoma patients, although the underlying mechanisms for this correlation are unknown (10, 11). Metastasis is a complex multistep process wherein tumor cells are driven, in part by lack of oxygen and nutrients, to abandon their tissue of origin and colonize distant sites (12). For example, hypoxia has been shown to promote release of tumor cell-derived lysyl oxidase (LOX), a HIF1α target that remodels collagen in the extracellular matrix of remote sites, thereby contributing to the establishment of the “pre-metastatic niche”(13) in murine breast cancer models. Whether similar, or distinct, cellular mechanisms regulate sarcoma metastasis is as yet unknown.

Collagen is the most abundant structural component of the extracellular matrix (ECM) and is aberrantly regulated in cancer at the levels of expression, post-translational modification, deposition and degradation (14). Consistent with their mesenchymal origins, primary

sarcomas produce and secrete large amounts of collagen, generating extensive extracellular collagen “highways”. These networks act as support scaffolds, facilitating tumor cell migration toward blood vessels and promoting their ability to escape the primary lesion (15-21). Mature collagen is formed by a series of enzymatic post-translational modifications of immature collagen polypeptides (22-24), although the factors required to establish and maintain collagen networks in sarcomas are not clear. Recently, HIF1α has been shown to regulate expression of prolyl hydroxylases and the endoplasmic reticulum (ER)-associated enzyme procollagen-lysine, 2-oxoglutarate 5-dioxygenase (PLOD2), also referred to as lysyl hydroxylase 2 (LH2) (25, 26). The primary function of PLOD2 is the initiation of lysine hydroxylation of collagen molecules (27-29). Hydroxylysines form carbohydrate attachment sites and are essential for the stability of collagen crosslinks (reviewed in (22)). Crosslinked collagen assembles into a triple helix, departs the ER and is then cleaved for assembly into fibrils. Prolyl and lysyl hydroxylation are crucial for the formation of normal mature collagen. Mutations in *PLOD2* cause the autosomal recessive disorder, Bruck syndrome, in which patients suffer osteoporosis, scoliosis, and joint contractures due to underhydroxylated collagen I (29); however, very little is known about the role of PLOD2 in tumorigenesis. Furthermore, the majority of research investigating the contribution of collagen and collagen-modifying enzymes to metastasis has been performed on epithelial cell-derived tumors, primarily breast cancer(13, 30). These processes remain understudied in mesenchymal tumors, including sarcomas.

Here we investigate the role of HIF1α and PLOD2 in sarcoma using samples from human patients and genetically engineered mouse models that faithfully recapitulate key aspects of human UPS. We show that HIF1α-dependent upregulation of PLOD2, but not LOX, is observed in metastatic human sarcomas, and is essential for the creation of collagen networks in primary murine tumors and subsequent metastasis to the lung. Importantly, Minoxidil-mediated PLOD inhibition decreased pulmonary metastasis in our murine allograft sarcoma model, suggesting that PLOD inhibition may prove a useful therapeutic intervention. Our findings indicate that intratumoral hypoxia and HIF1α-dependent *PLOD2* transcription promote sarcoma metastasis by modifying the collagen component of the ECM in primary tumors, and stimulating sarcoma cell migration. Furthermore, these data indicate that HIF1α confers distinct, tumor type-dependent effects on metastasis. Specifically, whereas HIF1α-driven LOX and PLOD2 expression have been shown to modify the premetastatic niche in breast cancers (13, 31), PLOD2, but not LOX, modifies the collagen network in primary sarcomas, with consequent effects on tumor cell migration and metastasis. Finally, we have demonstrated that PLOD2 is a credible and druggable therapeutic target in pre-metastatic sarcoma.

Results

Elevated HIF1α and PLOD2 correlate with sarcoma metastasis, but not primary tumor formation, in human and autochthonous murine tumors

To determine if *HIF1α* dependent upregulation of *PLOD2* could promote metastasis in primary human sarcomas, we compared relative gene expression based on microarray analysis of human metastatic and non-metastatic UPS and fibrosarcomas obtained prior to therapeutic intervention (32). *HIF1α* and *PLOD2* expression was selectively elevated in metastatic tumors (Fig. 1A; left and middle panels); in contrast, expression of *PLOD1,* a closely related isoform of *PLOD2*, and lysyl oxidase (*LOX*), another HIF1α transcriptional target and collagen-modifying enzyme, was not significantly altered (data not shown). Furthermore, qRT-PCR analysis of RNA obtained from an independent cohort of human UPS tumors showed that *PLOD2* levels are significantly higher in metastatic tumors relative to those that failed to metastasize (Fig. 1A, right panel). These data suggest that HIF1α-mediated *PLOD2* expression is associated with sarcoma metastasis.

We employed the genetically engineered murine *LSL-Kras$^{G12D/+}$; Trp53$^{fl/fl}$* (KP) model of UPS (8, 9) to investigate the effects of HIF1α and its target genes on soft tissue sarcoma development. In this model, injection of Adenovirus expressing Cre recombinase (Adeno-Cre) into the left gastrocnemius muscle results in *Kras^{G12D}* expression and *Trp53* deletion, producing sarcomas within approximately 8 weeks. We also crossed KP mice to *Hif1α$^{fl/fl}$* animals to generate the *LSL-Kras$^{G12D/+}$*; *Trp53$^{fl/fl}$*; *Hif1α$^{fl/fl}$* "KPH" strain, in which HIF1α is deleted in the Kras^{G12D}-expressing, p53-defiicent tumors. Genetic analysis showed highly effective Cre-dependent recombination of *Hif1α$^{fl/fl}$* alleles in the resulting sarcomas (Fig. 1B). KP and KPH animals developed tumors of similar size and latency indicating that loss of HIF1α did not alter primary tumor formation (Fig.1C) or growth (Fig. 1D). However, HIF1α deletion dramatically reduced the occurrence of pulmonary metastasis in this model, indicating that HIF1α specifically modulates tumor cell dissemination in sarcomas (Fig. 1E). Analysis of primary sarcomas by Masson's Trichrome staining of KP and KPH tumors revealed that HIF1α deletion significantly alters deposited collagen (Fig. 1F). No collagen fibers were found intersecting blood vessels in KPH tumors, whereas in KP tumors long strands of collagen with associated tumor cells were observed invading the vasculature (arrow, Fig.1F). Of note, HIF1α loss had no significant effect on sarcoma vessel density or perfusion (Supplementary Fig.1A), indicating that the vasculature is unaffected. These data suggest that the vasculature in KPH tumors is functioning similarly to control KP tumors and is unlikely to be responsible for the decrease in KPH metastasis. Picrosirius red staining revealed that HIF1α deletion has an unexpected effect on collagen organization (Fig. 1F, bottom panels). The collagen found in KPH tumors emits red birefringence, indicating higher levels of organization, while KP tumors contain collagen emitting green birefringence indicating that is more "immature". Processed mature collagen emits red birefringence in normal tissues (33). However, collagen organization/maturity can be aberrant in tumors, as indicated by green birefringence (34). Furthermore, collagen organization has been shown to decrease (change birefringence gradually from red to green) as tumors worsen in stage and grade (34). Picrosirius staining of normal tissue (Supplemental Fig.1B; white arrow) adjacent to KP tumors (black arrow) clearly shows the strong red/orange birefringence associated with normal collagen (blue arrow) in muscle tissue (white arrow). The lack of mature collagen organization in KP tumors is consistent with the idea that normal collagen modification and processing is disrupted due to elevated HIF1α/PLOD2 activity.

Collectively, these findings suggest that the loss of HIF1α alters collagen fiber deposition in primary sarcomas, and that PLOD2 may be a critical downstream target. To quantify the levels of PLOD2 in control and HIF1α-deficient sarcomas we derived cell lines from KP and KPH tumors. HIF1α and PLOD2 were elevated in KP cells exposed to hypoxia (0.5% O_2) for 16 hours, whereas KPH cells did not express HIF1α or PLOD2 under these conditions (Fig. 1G). A longer exposure of the western blot analyzing HIF1α and PLOD2 expression at 21% O_2 clearly shows that both proteins are expressed under normoxic conditions (Supplemental Fig. 1C), but are dramatically upregulated in response to hypoxia. Finally, qRT-PCR showed that *Plod2* mRNA levels were increased in hypoxic KP (KP1 and KP2) cells but not in KPH cells (KPH1 and KPH2) (Fig. 1H). Therefore, *Plod2* appears to be a HIF1α-regulated target on KP tumors and cells.

To demonstrate that our results were not unique to a specific genetic background, we investigated tumor cell lines derived from a distinct mouse model of sarcoma, *LSL-Kras$^{G12D/+}$; Ink4a/Arf$^{fl/fl}$* "KIA". Sarcomas initiated by Adeno-Cre injection into KIA mice display similar growth kinetics and histopathology as in KP mice (8). We confirmed that PLOD2 is also a hypoxia-induced HIF1α target in KIA cells (Fig. 1I). Quantification of 3 independent western blots showed that PLOD2 was significantly upregulated under hypoxia (P= 0.0118) (data not shown). Deletion of HIF1α using lentiviral-mediated shRNA

significantly abrogated hypoxia-induced PLOD2 expression (P= 0.0008). Similar results were obtained using the human fibrosarcoma cell line, HT-1080 (Fig. 1J). Quantification of 3 independent western blots showed that PLOD2 was significantly upregulated under hypoxia (P= 0.0301) (data not shown) and deletion of HIF1α significantly abrogated hypoxia-induced PLOD2 expression (P= 0.0095). qRT-PCR analyses of KIA (Fig. 1K) and HT-1080 (Fig. 1L) cells recapitulated these observations and showed that HIF1α regulates PLOD2 at the mRNA level. We concluded that HIF1α regulates *PLOD2* expression in human and murine sarcoma cells, and alters collagen deposition in primary murine sarcomas.

HIF1α and PLOD2 are required for metastasis in sarcoma

To establish a role for the HIF1α/PLOD2 pathway in sarcoma metastasis, we initially performed tail vein injections using 100,000 HT-1080 cells transduced with lentivirus expressing Scr, *HIF1α*, or *PLOD2* shRNA (Supplemental Fig. 1D,E). Silencing either *HIF1α* or *PLOD2* significantly inhibited HT-1080 cell lung colonization, suggesting a role for this pathway in sarcoma pulmonary metastasis. To further explore potential contributions of HIF1α to sarcomagenesis and metastases, we injected KIA (Supplementary Fig.2A-C) and HT-1080 (Supplementary Fig. 2D,E) cells subcutaneously into nude mice. We observed no significant change in primary tumor volume or weight. Subsequently, we performed similar experiments in KIA cells harboring PLOD2 shRNA for comparison to those treated with Scr or HIF1α shRNA (Fig. 2A). Although the mean weight of PLOD2-deficient tumors was slightly higher than that of control or HIF1α-deficient tumors (Fig. 2B), no differences in tumor volume were observed between groups (Fig. 2A), demonstrating that HIF1α and PLOD2 have little effect on primary tumor growth. However, silencing HIF1α or PLOD2 caused a striking reduction in lung metastases in KIA transplanted tumors (Fig. 2C,D,E)., indicating that the HIF1α /PLOD2 axis is necessary for pulmonary metastasis. HIF1α ablation did not affect the expression of related HIF1α targets, other than *Plod2*, including *Lox, Serpine 2, Col5a1,* and *Itgav* in HIF1α-depleted KIA tumors (data not shown) and cultured cells (Supplementary Fig. 2F). We confirmed that KIA tumors are hypoxic using Hypoxyprobe and HIF1α staining. Serial sectioning of KIA tumors showed that hypoxic regions circumscribe more oxygenated cells surrounding blood vessels, which can be visualized by Lectin staining (arrows, Fig. 2F). Importantly, picrosirius red staining of these tumor sections revealed that collagen is more organized in HIF1α /PLOD2 deleted tumors (Fig. 2G), consistent with analyses of KP and KPH primary tumors (Fig. 1F). Similarly, deletion of HIF1α and PLOD2 promoted the appearance of high molecular weight collagen I dimer (**) and trimer (***) structures, based on western blot analyses (Fig. 2H [16 hr] and Supplementary Fig. 2G [48 hr]). Normal collagen production requires the assembly of individual α chain collagen molecules into organized and post-translationally modified triple helix structures (22). We have observed that KP sarcoma cells lack these trimer structures, and dimer intermediates, in favor of monomeric collagen I. Deletion of the HIF1α/PLOD2 pathway allows normal maturation to occur in these cells. Interestingly, a recent study examining mutations involved in Bruck syndrome and osteogenesis imperfecta has shown that biallelic mutations in *PLOD2* promote collagen I trimer formation in patient-derived dermal fibroblasts (35). This finding is consistent with our observation that deletion of HIF1α-mediated PLOD2 expression promotes the formation of higher order collagen I structures. The changes we observe in collagen organization may be due to alterations in post-translational modifications found on collagen. Deletion of HIF1α and PLOD2 results in increased hydroxyproline levels in KIA tumors (Fig.2I), indicating that a high level of PLOD2 activity, resulting in elevated lysine hydroxylation, suppresses proline hydroxylation and mature “normal” collagen organization. Therefore, HIF1α/PLOD2 deletion allows for increased prolyl hydroxylation, stabilizing mature collagen organization. Based on these data, we conclude that HIF1α-mediated PLOD2 expression is not essential for primary

sarcoma tumor growth, but is required for efficient lung metastasis through effects on collagen maturation.

HIF1α and PLOD2 specifically control sarcoma cell migration

HIF1α and collagen deposition are known to promote metastasis by regulating tumor cell migration and invasion (13, 15, 30, 36, 37). We hypothesized that HIF1α might regulate these processes in sarcomas through upregulation of *PLOD2* transcription. Boyden chamber based migration assays, using immunoflourescent staining of migratory cell nuclei with 4',6-diamidino-2-phenylindole (DAPI), showed that shRNA-mediated knockdown of HIF1α and PLOD2 significantly decreased sarcoma cell motility under hypoxia in KP (Supplementary Fig. 3A), KIA (Supplementary Figure 3B), and HT-1080 cells (Supplementary Figure 3C). The HIF1α and migration findings are consistent with data presented by Kim et al., (38). Loss of KP cell motility due to HIF1α and PLOD2 deletion under normoxic conditions (Supplemental Fig. 3A) can be attributed to the presence of both proteins at 21% O_2 (Supplemental Fig. 1C).

It is well established that HIF1α can influence cell migration by modulating multiple cell-intrinsic effectors, including the expression of Snail and Twist (36, 37, 39). We reasoned that if altering extracellular collagen deposition was the primary effect of HIF1α on sarcoma cell migration, then the presence of wild type sarcoma cells should rescue defects in matching HIF1α-deficient cells in *in vitro* migration assays. To test this directly, we performed scratch migration assays using stable Scr, HIF1α-deficient, and PLOD2-deficient cells transduced with lentivirus bearing a dsRed expression vector (Scr shRNA) or a copGFP expression vector (HIF1α shRNA, PLOD2 shRNA). Migration of HIF1α-deficient copGFP+ cells and PLOD2-deficient copGFP+ cells was significantly delayed compared to control Scr dsRed cells in the KIA (Fig.3 A,B), KP (Supplementary Fig.4A,B), and HT-1080 cell lines (Supplementary Fig. 5A,B). However, when control and knockdown cells were mixed together, migration of both HIF1α-deficient and PLOD2-deficient cells were restored to control levels (Fig. 3A). Expression of copGFP and dsRED did not affect the ability of HIF1α to modulate PLOD2 levels in any of the three cell types (Fig. 3C, Supplementary Fig. 4C, and Supplementary Fig. 5C). Importantly, deletion of HIF1α and PLOD2 did not effect proliferation in these cell lines (Fig. 3D and Supplementary Fig. 5D). These data indicate that HIF1α drives sarcoma cell migration in a cell-extrinsic manner, possibly through PLOD2-mediated effects on collagen modification.

To determine whether HIF1α-mediated migration and invasion were PLOD2-dependent, we ectopically expressed PLOD2 in HIF1α-deficient KIA (Fig. 4A) and HT-1080 cells (Fig. 4B,C). HIF1α-deficient HT-1080 and KIA cells were transduced with control lentivirus or lentivirus bearing a wild-type PLOD2 expression vector. Western blot analysis showed endogenous and exogenous PLOD2 levels, as well as the efficacy of HIF1α inhibition (Supplementary Fig. 6A). Murine *Plod2* was expressed in human HT-1080 cells, and human *Plod2* in murine KIA cells, making it possible to evaluate changes in endogenous and ectopic PLOD2 mRNA levels by qRT-PCR using species-specific primers (Supplementary Fig. 6B). PLOD2 expression rescued cell migration in HIF1α-deficient cells under hypoxic conditions and also stimulated migration in normoxic cells (Fig. 4A,B, C). Interestingly, PLOD2 did not rescue invasion in KIA (Fig. 4D,F) or HT-1080 cells (Fig. 4E), warranting further *in vitro* and *in vivo* investigation (see below).

PLOD2 lysyl hydroxylase activity is required for sarcoma cell migration

PLOD2 lysyl hydroxylase activity is dependent upon association with several essential cofactors, including Fe^{2+} and 2-oxoglutarate, which requires a conserved aspartate residue (D689 in human PLOD2; D668 in mouse), and mutation of these amino acids inactivates

PLOD2 (27, 28). Using site-directed mutagenesis, we generated inactive PLOD2 (D689A, D668A) to determine if the enzymatic activity of PLOD2 was essential for its ability to rescue cell migration in HIF1α-deficient cells. We performed migration assays on stable Scr control and HIF1α-deficient HT-1080 and KIA cells that had also been transduced with lentivirus bearing a mutant PLOD2 expression vector. We observed that expression of inactive PLOD2 mutants failed to rescue migration in HIF1α-deficient KIA (Fig.5A) and HT-1080 cells (Fig. 5B). Furthermore, mutant PLOD2 behaves as a dominant negative in KIA and HT-1080 cells, suppressing hypoxia-induced migration. Interestingly, significant overexpression of mutant PLOD2 modestly inhibited endogenous PLOD2 and HIF1α levels as shown by qRT-PCR (Supplementary Fig. 6C,D) and western blot analysis (Supplementary Fig. 6E).

To confirm that PLOD2 is required for sarcoma cell migration, we used a previously described pharmacological inhibitor of PLOD2 expression, Minoxidil (40). Minoxidil treatment (0.5 mM) for 12 hours significantly reduced HT-1080 cell migration (Fig. 5C,D), concomitant with reduced PLOD2 protein levels as shown by western blot analysis of HT-1080 and KIA cells (Fig. 5E). Interestingly, Minoxidil increased HIFα levels, but not cell migration, supporting the conclusion that HIF1α-dependent induction of PLOD2 lysl hydroxylase activity is required for sarcoma cell migration. To determine the physiological importance of Minoxidil as a sarcoma metastasis inhibitor, we generated allografts of subcutaneously injected KIA cells in nude mice and immediately began injections of PBS, 1mg/kg Minoxidil, or 3 mg/kg Minoxidil every other day for 3 weeks. Minoxidil had no effect on primary tumor volume, tumor weight, or overall animal health/weight (Fig.5F and Supplementary Fig. 7A,B). However, Minoxidil treatment signficantly reduced the number of pulmonary metastases (Fig. 5G,H). Consistent with our observations in the autochthonous model, Minoxidil treated tumors contained relatively organized collagen compared with control treated tumors, based on picrosirius red birefringence (Fig.5I). These data demonstrate the potential usefulness of Minoxidil as a treatment for pre-metastatic sarcoma.

In vivo metastasis requires HIF1α/PLOD2-mediated collagen production

We tested the hypothesis that HIF1α-dependent PLOD2 expression and collagen modification are required for cell migration and metastasis *in vivo* using the KIA tumor transplant model of metastatic UPS. Staining of HIF1α-deficient tumor sections with Masson's Trichrome revealed a significant change in collagen staining, confirming that collagen was altered in the absence of HIF1α (Fig. 6A,B). Collagen was quantified using ImagePro7 software, which revealed a dramatic shift in collagen density in HIF1α-deficient tumors compared with control tumors (Fig. 6C). Intriguingly, HIF1α-deficient tumor cells appear smaller and rounder than control cells, which may reflect their relative inability to associate with and migrate along collagen fibers. To investigate this possibility, we performed second harmonic generation (SHG) analysis of explanted control and HIF1α-deficient tumors (Fig.6A,B). SHG imaging permits the co-visualization of endogenous collagen (red) and GFP+ tumor cells (green) in live tissue. In control tumors, we identified areas of highly branched/complex collagen and observed that GFP+ tumor cells associate closely with collagen and their morphology is elongated as they adhere to the fibers. In contrast, HIF1α-deficient tumors lack complex highly branched collagen deposits and tumor cells do not elongate or associate with the collagen that remains (Fig. 6A-C). Furthermore, HIF1α deletion causes a four-fold decrease in % collagen area (Figure 6C) and a concomitant four-fold decrease in murine lung metastasis (Figure 2D, middle). We conclude from these observations that there is a correlation between HIF1α-mediated collagen modification and metastasis. PLOD2-deficient tumors also possess defects in collagen maturation and cellular morphology, phenocopying what is seen when HIF1α is silenced (Fig. 6D). In many epithelial tumors, mesenchymal cells like fibroblasts are recruited and

subsequently secrete collagen. However, we reasoned that in mesenchymal lesions, the tumor cells themselves would likely perform this function. Therefore, we sought to determine whether a fibroblast population depositing additional collagen was present in our sarcoma model. Immunofluorescence anaylsis of GFP+ KIA tumor sections stained for GFP and the mesenchymal marker, Vimentin, showed that a small percentage of cells in the tumor were GFP-; Vimentin+ as expected for an infiltrating fibroblast population (Supplementary Fig. 8A). We quantified this population by flow cytometry using single cells suspensions of dissociated GFP+ tumors. Roughly 12% of cells in these tumors were GFP- infiltrating cells (Supplementary Fig. 8B). These data suggest that the tumor cells themselves (and not additional stromal cells) deposit the majority of collagen secreted in sarcomas.

Perhaps the most important aspect of collagen-associated tumor cell migration is the ability of the collagen network to deliver cells to the vasculature. To determine if this process is compromised in HIF1α-deficient sarcomas, we quantified the instances where collagen invades blood vessels in the tumors. In the absence of HIF1α, the loss of collagen at the blood vessels was severe (Fig. 6B). These findings are consistent with the overall conclusion that loss of HIF1α prevents tumor cells from migrating to vessels and escaping the primary lesion. PLOD2 ablation results in defects in collagen/vessel association similar to that of HIF1α-deficiency (Fig. 6B,D). Masson's Trichrome staining of Minoxidil treated tumors showed results similar to that of HIF1α and PLOD2-deficient tumors (Fig. 6E). Deposited collagen appears thinner and does not penetrate the vasculature, preventing tumor cells from using the collagen “highway” to disseminate to distant sites.

PLOD2 expression rescues *in vivo* metastasis of HIF1 α-deficient primary sarcomas

In order to clearly show that HIF1α-mediated regulation of PLOD2 is essential for metastasis, we performed an *in vivo* rescue experiment in which wild-type PLOD2 was ectopically expressed in HIF1α-deficient tumors (Fig. 7A,B,C). Expression of PLOD2 markedly rescued metastatic potential in KIA tumors (Fig. 7B,C), while having no reproducible effect on primary tumor volume (Fig. 7A). Given that PLOD2 promotes *in vivo* metastasis (Fig. 7A,B) and is required for lung colonization in a tail-vein injection assay (Supplementary Fig. 1D,E), we surmised that PLOD2 likely plays a critical role during *in vivo* blood vessel intravasation and extravasation, but this function is not assayable using standard Matrigel-coated transwell invasion inserts. PLOD2 may be required for tumor cell adhesion to vessels or cell survival while traveling in the vasculature. As stated above, neither HIF1α nor PLOD2 knockdown had any significant effect on proliferation in either cell type over a 3-day period (Fig. 3D and Supplementary Fig. 5D). Thus, we conclude that HIF1α and PLOD2 regulate multiple aspects of metastasis (migration, attachment to collagen networks, and vessel invasion).

Discussion

Soft tissue sarcomas are a highly complex set of malignancies, comprising more than 50 histologically distinct subtypes associated with genetic alterations in diverse molecular pathways (5). Although lethal metastases, particularly to the lung, are a common occurrence in sarcoma patients, the molecular mechanisms regulating this process are largely unknown. Primary sarcomas are noted for extensive fibrosis and deposition of extracellular matrix components, a feature that has been associated with metastatic potential in numerous cancers (41, 42). Although many details are incompletely understood, it is clear that metastatic tumor cells can associate physically with dense collagen networks in solid tumors, and migrate along this collagen “highway” toward vascular tissues (18, 43), through which they ultimately disseminate and colonize distant organs. Therefore, therapeutic manipulation of collagen modification/organization in primary sarcomas, as well as other tumors, could have

significant impact on an early, proximal step in metastasis, which remains the leading cause of cancer-related death.

Low intratumoral O_2 levels and HIF1α expression are key predictors of metastatic potential in sarcomas. Although previous microarray analyses revealed elevated *HIF1α* and *PLOD2* expression in sarcoma patient samples (32), the mechanisms by which these genes regulate sarcoma progression and/or metastasis were unclear. In this study, we demonstrate that *HIF1α* and *PLOD2* expression levels are preferentially elevated in primary human sarcomas that subsequently metastasized, suggesting they regulate one or more aspect of tumor cell dissemination. Using independent murine sarcoma models, we determined that HIF1α-dependent PLOD2 expression is required for deposition of the disorganized collagen required to facilitate tumor cell migration in primary tumors, as well as pulmonary metastasis. *In vitro* assays revealed that the HIF1α/PLOD2 pathway regulates sarcoma cell migration in a collagen-dependent manner. Finally, ectopic expression of PLOD2 rescues both cell migration and metastatic potential in HIF1α-deficient cells and tumors. Collectively, our data indicate that HIF1α-dependent PLOD2 expression is essential for hypoxia-mediated collagen disorganization and metastasis in sarcomas (see model in Fig. 7D). Unexpectedly, we conclude that disorganized/immature collagen take on a denser structure and are alternately modified in a way that supports tumor cell adherence and migration. Deletion of HIF1α collagen modification and organization, preventing its association with tumor cells.

It is important to note that HIF1α regulates multiple, distinct pathways associated with metastasis in various tumor models. For example, HIF1α reduces E-cadherin expression and promotes invasiveness and the epithelial to mesenchymal transition (EMT) in renal cancers (44). Moreover, HIF1α enhances metastasis by regulating *TWIST1* transcription in head and neck squamous cell cancers (36, 37). However, in our sarcoma models *Twist1* and *Snail* expression, were found to be insensitive to hypoxic stimulation (data not shown) making them less likely to contribute to hypoxia-mediated migration and invasion. HIF1α has also been shown to play important cell-extrinsic roles in breast cancer models, where it induces expression of ECM modifying enzymes, which promotes effective metastasis by modifying the pre-metastatic niche (13, 31). Additionally, HIF1α-dependent expression of prolyl hydroxylases as well as Angiopoietin-like 4 and L1CAM promotes breast cancer metastasis by controlling tumor cell invasion of the vasculature (45, 46). In primary sarcomas, HIF1α-dependent PLOD2 expression has a profound effect on extracellular collagen networks, which in turn regulate tumor cell migration and the initiation of metastasis. Interestingly, PLOD2 has been recently identified as a novel prognostic factor in hepatocellular carcinoma, in which it is associated with disease recurrence and intrahepatic metastases (47). Although previous work from multiple groups has highlighted the importance of collagen as a scaffold that supports the migration of metastatic tumor cells (18, 43), the cellular processes that create these collagen deposits are relatively understudied.

As hypoxia and HIF expression are important prognostic indicators in many solid tumors, conclusions drawn from the current studies may be applicable in multiple tumor contexts, although other collagen modifying enzymes, such as PLOD1 or LOX, may also contribute in other tumor types. In sarcoma, further investigation of PLOD2 as a feasible therapeutic target is clearly warranted. We have used the PLOD2 inhibitor, Minoxidil, to address the importance of PLOD2 in tumor cell migration and *in vivo* pulmonary metastases, although the usefulness of this drug in the clinic or as a lead compound for novel drug discovery remains to be determined.

Although metastases are responsible for the vast majority of cancer-associated deaths, there are very few therapeutic approaches that specifically target metastasis in any tumor model.

Based on our findings it seems prudent to pursue clinical agents that would inhibit metastasis by compromising the ECM network in conjunction with the current standard of therapy.

Methods

Gene expression analysis

RNA was isolated from human tumor tissue using RNeasy kit (Qiagen) and quality was analyzed using a 2100 Bioanalyzer (Agilent Technologies). Amplification was achieved using the TotalPrep RNA Amplification Kits (Illumina). Amplified cRNAs were then hybridized on HumanRef8 Expression Beadchips (Illumina), which target more than 24,000 genes. Image analysis was performed using Illumina's BeadStudio v3.0.14 Gene Expression Module. All statistical analyses were done using the statistical software R (http://www.r-project.org). Supervised hierarchical clustering of 140 genes transcriptionally regulated by HIF1α was performed using 1-r (Pearson correlation) as a distance metric with a complete linkage. Data from this analysis was used to determine relative gene enrichment.

Mouse models

Generation of *Hif1a*$^{fl/fl}$ mice (48) and *LSL-Kras*$^{G12D/+}$*Trp53*$^{fl/fl}$ mice has been previously described (8). These mice were crossed to create the *LSL-Kras*$^{G12D/+}$*Trp53*$^{fl/fl}$*Hif1a*$^{fl/fl}$ animals. Soft tissue sarcomas were generated by intramuscular injection of a calcium phosphate precipitate of Ad-Cre (Gene Transfer Vector Core, University of Iowa). For transplant tumors 1×10^6 KIA (derived from *LSL-Kras*$^{G12D/+}$*Ink4a*$^{fl/fl}$ tumors) were injected subcutaneously into the flanks of nu/nu mice (Charles River Laboratories). In each experiment 10 mice per experimental group were used with each mouse bearing two subcutaneous tumors. Tumors developed after 3-5 days, were monitored every other day, and animals were euthanized after 20-30 days. For *in vivo* lung metastasis analysis lung tissues were removed, and sections were stained with hematoxylin and eosin. Images were acquired using a Nikon SMZ800 stereoscope with a Nikon 1200F digital camera and Nikon Act-1 software. The ratio of total metastatic sarcoma foci to total lung area (% tumor burden) was determined using ImagePro 6.3 software (Media Cybernetics Inc.). Additionally, the percent of animals in the entire cohort with metastatic foci was evaluated along with total number of metastatic foci per experiment and the averae number of sarcoma lung foci per lung in each experiment. For Minoxidil injections, allografts and drug treatments were started simultaneously. Mice bearing subcutaneous KIA tumors on each flank were intraperitoneal injected with PBS, 1mg/kg Minoxidil, or 3 mg/kg Minoxidil every other day unless the animals were euthanized, the tumors and lungs removed.

Cell Culture, treatment and Lentiviral transduction

HT-1080 cells were purchased from ATCC (Manassas, VA) January 8, 2010. The cells were authenticated by karyotyping and DNA profiling from the initial seed stock. KIA cells were derived in the laboratory from *LSL-Kras*$^{G12D/+}$*Ink4a*$^{fl/fl}$ tumors as described elsewhere (8, 49). Finally, KP1 and KP2 were derived from *LSL-Kras*$^{G12D/+}$*Trp53*$^{fl/fl}$ tumors and KPH1 and KPH2 cells were derived from *LSL-Kras*$^{G12D/+}$*Trp53*$^{fl/fl}$*Hif1a*$^{fl/fl}$ tumors. Low-oxygen conditions were achieved in a Ruskinn in vivo$_2$ 400 work station. Cells were treated with 0.5 mM Minoxidil diluted in DMEM culture media (Sigma Aldrich) for 36-48 hrs, and drug was replenished every 24 hrs. For shRNA-mediated knockdown of *Hif1α, HIF1α, Plod2,* and *PLOD2* lentiviral particles bearing pLKO.1 shRNA plasmids were generated in HEK-293T cells. 293T cells were transfected overnight with pLKO.1 empty vector, nonspecific shRNA, or target-specific shRNA and viral packaging plasmids, according to the Fugene reagent protocol (Roche). The following shRNA pLKO.1 plasmids were employed: pLKO.1 scrambled shRNA (Addgene 1864), pLKO.1 *Hif1α* shRNA

(TRCN0000054448), pLKO.1 *HIF1α* shRNA (TRCN0000003808), pLKO.1 *Plod2* (TRCN0000076411), *PLOD2* (TRCN0000064809) (Thermofisher Scientific), G protein of vesicular stomatitis virus (VSV-G), pMDLG, pRSV-rev. Supernatant was harvested from cultures at 24 hrs and 48 hrs post-transfection, and virus concentrated using 10-kDa Amicon Ultra-15 centrifugal filter units (Millipore). Ectopic expression of wild type and mutant PLOD2 was achieved using pCDH-CMV-MCS-EF1-Puro expression vectors (System Biosciences) and were cloned in via Xba1 and NHE1 restriction sites from murine or human pCMV-SPORT6 PLOD2 (Open Biosystems). PLOD2 mutants were generated using the QuikChange II site-directed mutagenesis kit (Agilent Technologies). pLKO.1 shRNA and pCDH-CMV-MCS-EF1-Puro plasmids contain a puromycin resistance gene, thus transduction efficiency was evaluated by puromycin selection. Cells were used for assays 4 days postransduction. GFP was introduced using the pCDH-CMV-EF1-copGFP vector (System Biosciences). copGFP (copepod GFP) is particularly bright and thus is suitable for *in vivo* SHG studies as well as cell culture. dsRED was expressed from the pULTRA-HOT vector (Addgene plasmid# 24130) originally constructed by Didier Trono.

Immunostaining and Imaging

Immunohistochemistry of tissue sections with antibodies to HIF1MVα (Abcam) and Lectin (Vector Labs) was performed using enzymatic Avidin-Biotin Complex (ABC)-diaminobenzidine (DAB) staining (Vector Labs). Nuclei were counterstained with hematoxylin. Immunofluorescences staining of copGFP (Evrogen) and Vimentin (Abcam) as well as DAPI (Invitrogen) stained images were visualized using an Olympus IX81 microscope. Collagen was stained using Masson's Trichrome Kit (Sigma Aldrich) and nuclei were counterstained with Weigert's iron hematoxylin (Sigma Aldrich). Collagen second harmonic generation (SHG) images were captured using a Prairie Technologies Ultima 2-Photon Microscope system (Middleton, WI). Images were taken with an excitation wavelength of 910 nm, and captured through an emission filter of 457-487 nm (that detects the SHG signal for collagen). Collagen was quantified using Image-Pro software. All comparative images were obtained using identical microscope and camera settings. Picrosirius Red staining (Electron Microscopy Sciences) and analysis was conducted using paraffin sections of primary murine sarcomas stained with 0.1% picrosirius and counterstained with Weigert's Hematoxylin to visualize fibrillar collagen. Sections were imaged using a Leica DMRB microscope bearing an analyzer and polarizer (leica) and an Olympus DP72 camera.

Western Blotting, qRT-PCR, Hydroxyproline measurement

Whole cell lysates were prepared in SDS/Tris pH 7.6 lysis buffer. Proteins were electrophoresed and separated by SDS-PAGE and transferred to nitrocellulose membranes and probed with the following antibodies: rabbit anti-HIF1α (Cayman Chemical co.), rabbit anti-GAPDH (Cell Signaling Inc.), and rabbit anti-Collagen I (Millipore), rabbit anti-PLOD2 (Proteintech). Densitometry was performed using ImageJ software. Representative western blots from multiple independent experiments are presented. Total RNA was isolated from cells using the TRIzol reagent protocol (Invitrogen) and from tumor tissue using the RNAeasy minikit (Qiagen). mRNA was reverse transcribed using the High-Capacity RNA-to-cDNA kit (Applied Biosystems). Transcript expression was determined by quantitative PCR of synthesized cDNA using the Applied Biosystems 7900HT system. Target cDNA amplification was measured using TaqMan primer/probe sets (Applied Biosystems) for human and murine Hif1α, Plod2, HPRT1 (control), Lox, Serpine 2, Col5a1, and Itgav. Hydroxyproline was assessed using homogenized tumor samples and the Hydoxyproline Assay Kit (Biovision Inc.).

Migration, Invasion, and Proliferation assays

Migration assays were performed using 24-well chambers with inserts (8-μm pores) (BD Biosciences). Medium containing 10% serum was placed in the lower chamber, and tumor cells (1×10^5) suspended in medium without serum were added to the top chamber. The plates were incubated under 21% or 0.5% O_2 for 4 hrs (HT-1080) or 18 hrs (KIA). After migration, nonmigratory cells were removed from the top of the insert membrane using cotton swabs. The underside of each membrane was fixed in Methanol and stained with DAPI (Invitrogen), and the number of cells that migrated completely through the 8-μm pore was determined in 6 random high-power fields (20x objective) for each membrane. Invasion was examined in a similar way using Matrigel-coated inserts (BD Biosciences). Scratch assays were performed on confluent KP, KIA, and HT-1080 cells expressing either dsREd or copGFP and seed on to plates at a 1:1 ratio. Cells were imaged under normoxic conditions. ImageJ software was used to measure areas devoid of cells in 5 unique fields per condition. As cells migrated into the wounds, those areas became smaller. We determined the average area lacking GFP+ cells per condition and displayed those means as a normalized percentage with the pre-wounding image representing the baseline and then generated recovery statistics. Proliferation was assessed by counting cell numbers manually using a hemocytometer every day for 4 days.

Flow Cytometry

Tumors were dissected, homogenized and collagenase treated to generate a single cell suspension. Live cells were run on a BD LSR II flow cytometer for the detection of GFP. GFP negative parent cell lines were also run to set up GFP+ and GFP- gates.

Statistical Analysis

Data are represented as mean ± SEM. Unpaired 2-tailed Student's *t* test was preformed for most of the studies to evaluate the differences between the control and experimental groups. $P \leq 0.05$ was considered statistically significant. Significance is indicated by the presence of an asterisk "*". Quantified data shown represent at least 3 independent experiments. GraphPad Prism software (La Jolla, CA) was used to conduct all statistical analyses.

Supplementary Material

Refer to Web version on PubMed Central for supplementary material.

Acknowledgments

The authors would like to thank J. Hayden and F. Kenney of the Wistar Institute Microscopy Core Facility for their assistance with imaging, as well as B. Krock and T. Richardson-Metzger for assistance with flow cytometry and mouse experiments, respectively. The authors also thank the following investigators for generously providing mouse strains: *LSL-Kras*$^{G12D/+}$ (T. Jacks, MIT), *Trp53*$^{fl/fl}$ (A. Burns, NKI), *Ink4a/Arf*$^{fl/fl}$ (R. DePinho, MD Anderson), *HIF1α*$^{fl/fl}$ (R. Johnson, Cambridge). This work was supported by the US National Cancer Institute grant F32 CA156979 (T.S.K.E.M), T32 CA09140, R01CA158301(T.S.K.E.M). (S.S.Y) (M.C.S.), and R01CA138265 (DGK). M.C.S. is an investigator of the Howard Hughes Medical Institute.

Financial Support

F32 CA156979, T32 CA09140 (T.S.K.E.M)

R01CA158301(T.S.K.E.M) (M.S.N) (T.K.) (V.M.) (J.E.S.S) (S.S.Y) (M.C.S.) (L.S.) (E.P.)

R01CA138265 (D.G.K.) (Q.Q.) (M.Z.)

Howard Hughes Medical Institute (M.C.S) (N.S.)

Abbreviations list

HIF1α	Hypoxia Inducible Factor 1α
PLOD2	procollagen-lysine, 2-oxoglutarate 5-dioxygenase 2
LOX	lysyl oxidase
UPS	Undifferentiated Pleomorphic Sarcoma
ECM	extracellular matrix
ER	endoplasmic reticulum
Scr	scramble

References

1. Jemal A, Siegel R, Xu J, Ward E. Cancer statistics, 2010. CA Cancer J Clin. 2010; 60:277–300. [PubMed: 20610543]
2. Italiano A, Mathoulin-Pelissier S, Cesne AL, Terrier P, Bonvalot S, Collin F, et al. Trends in survival for patients with metastatic soft-tissue sarcoma. Cancer. 2011; 117:1049–54. [PubMed: 20945333]
3. Soleimani VD, Rudnicki MA. New insights into the origin and the genetic basis of rhabdomyosarcomas. Cancer Cell. 2011; 19:157–9. [PubMed: 21316595]
4. Rubin BP, Nishijo K, Chen HI, Yi X, Schuetze DP, Pal R, et al. Evidence for an unanticipated relationship between undifferentiated pleomorphic sarcoma and embryonal rhabdomyosarcoma. Cancer Cell. 2011; 19:177–91. [PubMed: 21316601]
5. Taylor BS, Barretina J, Maki RG, Antonescu CR, Singer S, Ladanyi M. Advances in sarcoma genomics and new therapeutic targets. Nat Rev Cancer. 2011; 11:541–57. [PubMed: 21753790]
6. Helman LJ, Meltzer P. Mechanisms of sarcoma development. Nat Rev Cancer. 2003; 3:685–94. [PubMed: 12951587]
7. Matushansky I, Charytonowicz E, Mills J, Siddiqi S, Hricik T, Cordon-Cardo C. MFH classification: differentiating undifferentiated pleomorphic sarcoma in the 21st Century. Expert Rev Anticancer Ther. 2009; 9:1135–44. [PubMed: 19671033]
8. Kirsch DG, Dinulescu DM, Miller JB, Grimm J, Santiago PM, Young NP, et al. A spatially and temporally restricted mouse model of soft tissue sarcoma. Nat Med. 2007; 13:992–7. [PubMed: 17676052]
9. Mito JK, Riedel RF, Dodd L, Lahat G, Lazar AJ, Dodd RD, et al. Cross species genomic analysis identifies a mouse model as undifferentiated pleomorphic sarcoma/malignant fibrous histiocytoma. PLoS One. 2009; 4:e8075. [PubMed: 19956606]
10. Brizel DM, Scully SP, Harrelson JM, Layfield LJ, Bean JM, Prosnitz LR, et al. Tumor oxygenation predicts for the likelihood of distant metastases in human soft tissue sarcoma. Cancer Res. 1996; 56:941–3. [PubMed: 8640781]
11. Nordsmark M, Alsner J, Keller J, Nielsen OS, Jensen OM, Horsman MR, et al. Hypoxia in human soft tissue sarcomas: adverse impact on survival and no association with p53 mutations. Br J Cancer. 2001; 84:1070–5. [PubMed: 11308256]
12. Nguyen DX, Bos PD, Massague J. Metastasis: from dissemination to organspecific colonization. Nat Rev Cancer. 2009; 9:274–84. [PubMed: 19308067]
13. Erler JT, Bennewith KL, Nicolau M, Dornhofer N, Kong C, Le QT, et al. Lysyl oxidase is essential for hypoxia-induced metastasis. Nature. 2006; 440:1222–6. [PubMed: 16642001]
14. Lu P, Weaver VM, Werb Z. The extracellular matrix: a dynamic niche in cancer progression. J Cell Biol. 2012; 196:395–406. [PubMed: 22351925]
15. Egeblad M, Rasch MG, Weaver VM. Dynamic interplay between the collagen scaffold and tumor evolution. Curr Opin Cell Biol. 2010; 22:697–706. [PubMed: 20822891]

16. Wang W, Wyckoff JB, Frohlich VC, Oleynikov Y, Huttelmaier S, Zavadil J, et al. Single cell behavior in metastatic primary mammary tumors correlated with gene expression patterns revealed by molecular profiling. Cancer Res. 2002; 62:6278–88. [PubMed: 12414658]

17. Zaman MH, Trapani LM, Sieminski AL, Mackellar D, Gong H, Kamm RD, et al. Migration of tumor cells in 3D matrices is governed by matrix stiffness along with cell-matrix adhesion and proteolysis. Proc Natl Acad Sci U S A. 2006; 103:10889–94. [PubMed: 16832052]

18. Condeelis J, Segall JE. Intravital imaging of cell movement in tumours. Nat Rev Cancer. 2003; 3:921–30. [PubMed: 14737122]

19. Han S, Makareeva E, Kuznetsova NV, DeRidder AM, Sutter MB, Losert W, et al. Molecular mechanism of type I collagen homotrimer resistance to mammalian collagenases. J Biol Chem. 2010; 285:22276–81. [PubMed: 20463013]

20. Levental KR, Yu H, Kass L, Lakins JN, Egeblad M, Erler JT, et al. Matrix crosslinking forces tumor progression by enhancing integrin signaling. Cell. 2009; 139:891–906. [PubMed: 19931152]

21. Makareeva E, Han S, Vera JC, Sackett DL, Holmbeck K, Phillips CL, et al. Carcinomas contain a matrix metalloproteinase-resistant isoform of type I collagen exerting selective support to invasion. Cancer Res. 2010; 70:4366–74. [PubMed: 20460529]

22. Myllyharju J, Kivirikko KI. Collagens, modifying enzymes and their mutations in humans, flies and worms. Trends Genet. 2004; 20:33–43. [PubMed: 14698617]

23. Pihlajaniemi T, Myllyla R, Alitalo K, Vaheri A, Kivirikko KI. Posttranslational modifications in the biosynthesis of type IV collagen by a human tumor cell line. Biochemistry. 1981; 20:7409–15. [PubMed: 6798991]

24. Sipila L, Ruotsalainen H, Sormunen R, Baker NL, Lamande SR, Vapola M, et al. Secretion and assembly of type IV and VI collagens depend on glycosylation of hydroxylysines. J Biol Chem. 2007; 282:33381–8. [PubMed: 17873278]

25. Gilkes DM, Bajpai S, Chaturvedi P, Wirtz D, Semenza GL. Hypoxia-inducible factor 1 (HIF-1) promotes extracellular matrix remodeling under hypoxic conditions by inducing P4HA1, P4HA2, and PLOD2 expression in fibroblasts. J Biol Chem. 2013; 288:10819–29. [PubMed: 23423382]

26. Hofbauer KH, Gess B, Lohaus C, Meyer HE, Katschinski D, Kurtz A. Oxygen tension regulates the expression of a group of procollagen hydroxylases. Eur J Biochem. 2003; 270:4515–22. [PubMed: 14622280]

27. Rautavuoma K, Takaluoma K, Passoja K, Pirskanen A, Kvist AP, Kivirikko KI, et al. Characterization of three fragments that constitute the monomers of the human lysyl hydroxylase isoenzymes 1-3. The 30-kDa N-terminal fragment is not required for lysyl hydroxylase activity. J Biol Chem. 2002; 277:23084–91. [PubMed: 11956192]

28. Pirskanen A, Kaimio AM, Myllyla R, Kivirikko KI. Site-directed mutagenesis of human lysyl hydroxylase expressed in insect cells. Identification of histidine residues and an aspartic acid residue critical for catalytic activity. J Biol Chem. 1996; 271:9398–402. [PubMed: 8621606]

29. Hyry M, Lantto J, Myllyharju J. Missense mutations that cause Bruck syndrome affect enzymatic activity, folding, and oligomerization of lysyl hydroxylase 2. J Biol Chem. 2009; 284:30917–24. [PubMed: 19762917]

30. Erler JT, Giaccia AJ. Lysyl oxidase mediates hypoxic control of metastasis. Cancer Res. 2006; 66:10238–41. [PubMed: 17079439]

31. Wong CC, Zhang H, Gilkes DM, Chen J, Wei H, Chaturvedi P, et al. Inhibitors of hypoxia-inducible factor 1 block breast cancer metastatic niche formation and lung metastasis. J Mol Med (Berl). 2012

32. Detwiller KY, Fernando NT, Segal NH, Ryeom SW, D'Amore PA, Yoon SS. Analysis of hypoxia-related gene expression in sarcomas and effect of hypoxia on RNA interference of vascular endothelial cell growth factor A. Cancer Res. 2005; 65:5881–9. [PubMed: 15994966]

33. Singh HP, Shetty DC, Wadhwan V, Aggarwal P. A quantitative and qualitative comparative analysis of collagen fibers to determine the role of connective tissue stroma on biological behavior of odontogenic cysts: A histochemical study. Natl J Maxillofac Surg. 2012; 3:15–20. [PubMed: 23251052]

34. Aparna V, Charu S. Evaluation of collagen in different grades of oral squamous cell carcinoma by using the picrosirius red stain- a histochemical study. Journl of Clinical and Diagnostic Research. 2010; 4:3444–9.
35. Schwarze U, Cundy T, Pyott SM, Christiansen HE, Hegde MR, Bank RA, et al. Mutations in FKBP10, which result in Bruck syndrome and recessive forms of osteogenesis imperfecta, inhibit the hydroxylation of telopeptide lysines in bone collagen. Hum Mol Genet. 2013; 22:1–17. [PubMed: 22949511]
36. Yang MH, Wu KJ. TWIST activation by hypoxia inducible factor-1 (HIF-1): implications in metastasis and development. Cell Cycle. 2008; 7:2090–6. [PubMed: 18635960]
37. Yang MH, Wu MZ, Chiou SH, Chen PM, Chang SY, Liu CJ, et al. Direct regulation of TWIST by HIF-1alpha promotes metastasis. Nat Cell Biol. 2008; 10:295–305. [PubMed: 18297062]
38. Kim YJ, Lee HJ, Kim TM, Eisinger-Mathason TS, Zhang AY, Schmidt B, et al. Overcoming evasive resistance from vascular endothelial growth factor a inhibition in sarcomas by genetic or pharmacologic targeting of hypoxia-inducible factor 1alpha. Int J Cancer. 2013; 132:29–41. [PubMed: 22684860]
39. Mak P, Leav I, Pursell B, Bae D, Yang X, Taglienti CA, et al. ERbeta impedes prostate cancer EMT by destabilizing HIF-1alpha and inhibiting VEGF-mediated snail nuclear localization: implications for Gleason grading. Cancer Cell. 2010; 17:319–32. [PubMed: 20385358]
40. Zuurmond AM, van der Slot-Verhoeven AJ, van Dura EA, De Groot J, Bank RA. Minoxidil exerts different inhibitory effects on gene expression of lysyl hydroxylase 1, 2, and 3: implications for collagen cross-linking and treatment of fibrosis. Matrix Biol. 2005; 24:261–70. [PubMed: 15908192]
41. Kalluri R, Zeisberg M. Fibroblasts in cancer. Nat Rev Cancer. 2006; 6:392–401. [PubMed: 16572188]
42. Hanahan D, Coussens LM. Accessories to the crime: functions of cells recruited to the tumor microenvironment. Cancer Cell. 2012; 21:309–22. [PubMed: 22439926]
43. Roussos ET, Condeelis JS, Patsialou A. Chemotaxis in cancer. Nat Rev Cancer. 2011; 11:573–87. [PubMed: 21779009]
44. Krishnamachary B, Zagzag D, Nagasawa H, Rainey K, Okuyama H, Baek JH, et al. Hypoxia-inducible factor-1-dependent repression of E-cadherin in von Hippel-Lindau tumor suppressor-null renal cell carcinoma mediated by TCF3, ZFHX1A, and ZFHX1B. Cancer Res. 2006; 66:2725–31. [PubMed: 16510593]
45. Zhang H, Wong CC, Wei H, Gilkes DM, Korangath P, Chaturvedi P, et al. HIF-1-dependent expression of angiopoietin-like 4 and L1CAM mediates vascular metastasis of hypoxic breast cancer cells to the lungs. Oncogene. 2012; 31:1757–70. [PubMed: 21860410]
46. Gilkes DM, Bajpai S, Chaturvedi P, Wirtz D, Semenza GL. HIF-1 Promotes Extracellular Matrix Remodeling under Hypoxic Conditions by Inducing P4HA1, P4HA2, and PLOD2 Expression in Fibroblasts. J Biol Chem. 2013
47. Noda T, Yamamoto H, Takemasa I, Yamada D, Uemura M, Wada H, et al. PLOD2 induced under hypoxia is a novel prognostic factor for hepatocellular carcinoma after curative resection. Liver Int. 2012; 32:110–8. [PubMed: 22098155]
48. Ryan HE, Poloni M, McNulty W, Elson D, Gassmann M, Arbeit JM, et al. Hypoxia-inducible factor-1alpha is a positive factor in solid tumor growth. Cancer Res. 2000; 60:4010–5. [PubMed: 10945599]
49. Yoon SS, Stangenberg L, Lee YJ, Rothrock C, Dreyfuss JM, Baek KH, et al. Efficacy of sunitinib and radiotherapy in genetically engineered mouse model of soft-tissue sarcoma. Int J Radiat Oncol Biol Phys. 2009; 74:1207–16. [PubMed: 19545786]

Significance

Undifferentiated Pleomorphic Sarcomas (UPS) is a commonly diagnosed and particularly aggressive sarcoma subtype in adults, which frequently and fatally metastasizes to the lung. Here we demonstrate the potential utility of a novel therapeutic target for the treatment of metastatic UPS, specifically the collagen-modifying enzyme PLOD2.

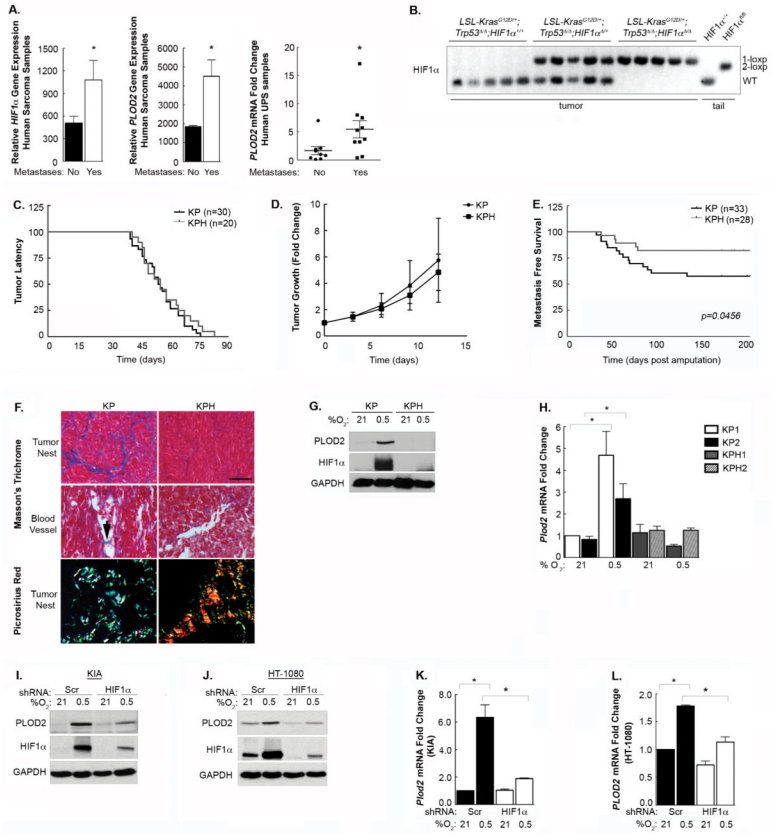

Figure 1. HIF1α is an important regulator of metastasis in an autochthonous, genetic model of UPS potentially via PLOD2 modulation

(A) (Left and Middle Panels) Relative gene expression in human metastatic (N=5) and non-metastatic (N=8) UPS and fibrosarcoma in patients treated as Massachusetts General Hospital (32). *HIF1α* (*P*=0.0312) and *PLOD2* (*P* =0.0011) were significantly upregulated in metastatic sarcomas. **(Right Panel)** qRT-PCR analysis of 10 human UPS patient samples treated at the University of Pennsylvania; *P=0.044.* **(B)** Mouse models of sarcoma. *LSL-Kras*$^{G12D/+}$*;Trp53*$^{fl/fl}$ (KP) and *LSL-Kras*$^{G12D/+}$*;Trp53*$^{fl/fl}$*;Hif1α*$^{fl/fl}$ (KPH) genotyping showed effective recombination of *Hif1α*^{fl} alleles in Adeno-Cre initiated tumors. **(C)** Mice remained tumor free for roughly 40 days, by 90 days all of the mice had developed palpable tumors (volume= 200mm^3) KP; *n*=30, KPH; *n*=20; (P=0.3755). **(D)** Primary tumor size. Two weeks after tumors were palpable they had grown 2-8 fold larger, but there was no difference between KP; *n*=7 and KPH; *n* =9 tumor growth (*P*=0.7342) **(E)** Metastasis free survival in KP; *n*=33 and KPH; *n*=28 mice; *P*=0.0456. Lung metastases were confirmed histologically. **(F)** Masson's Trichrome and picrosirius red staining of tumor nest areas and blood vessels in primary KP and KPH tumors. Deletion of HIF1α alters collagen in KPH tumors. Masson's Trichrome stains collagen fibers blue. Cells were counterstained in red with Weigert's hematoxylin. (Scale bar;50 μm). **(G)** Western blot analyses of sarcoma cells derived from KP and KPH tumors. Expression of HIF1α and PLOD2 proteins is hypoxia inducible and abolished when HIF1α is deleted. **(H)** qRT-PCR analysis of 2 individually derived KP and KPH cell lines. *Plod2* mRNA transcription is induced under hypoxic conditions in control cells (KP1; *P* =0.0284 and KP2; *P* =0.0391). Deletion of HIF1α abolished hypoxia-induced *Plod2* mRNA levels. **(I)** Western blot of PLOD2 expression in KIA cells and **(J)** HT-1080 cells. **(K)** qRT-PCR analyses of KIA cells. Expression of *Hif1α* and *Plod2* is hypoxia inducible (*Plod2* qRT-PCR: *P* =0.0284) and is abolished when HIF1α is deleted (*Plod2* qRT-PCR: *P* =0.0403). **(L)** HT-1080 cells were evaluated by qRT-PCR as

in (K). Expression of *Hif1α* and *Plod2* is hypoxia inducible (*Plod2* qRT-PCR: $P = 0.0006$) and is abolished when HIF1α is deleted (*Plod2* qRT-PCR: $P = 0.0210$).

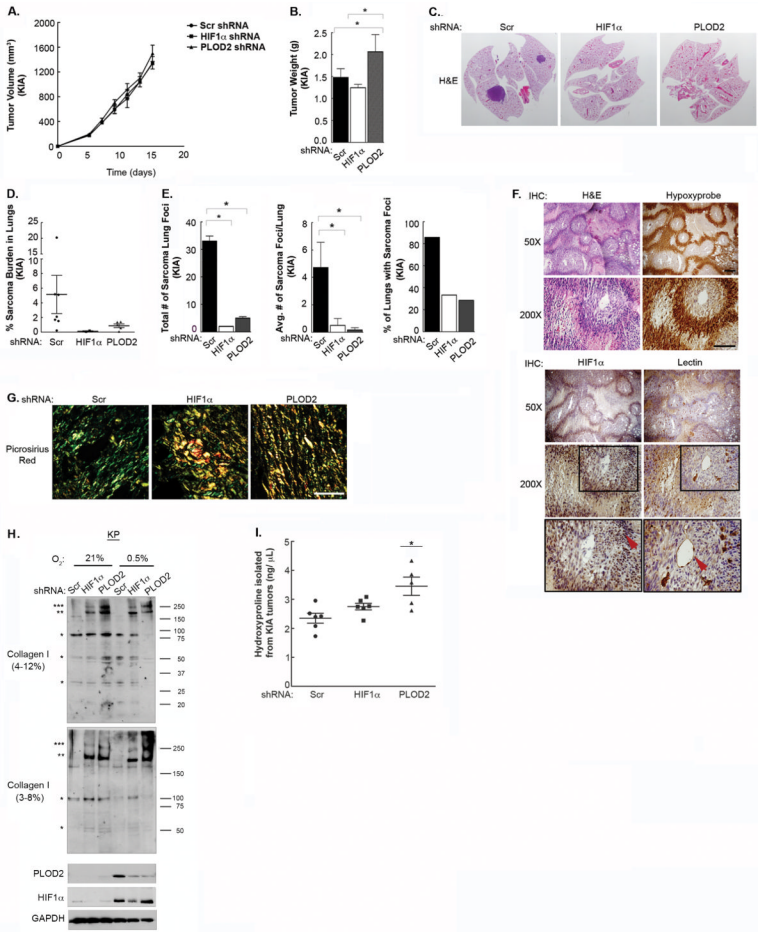

Figure 2. HIF1α and PLOD2 are dispensable for primary sarcoma formation but essential for metastasis

(A) Tumor allograft using 1×10^6 Scr, HIF1α-deficient, or PLOD2-deficient KIA cells subcutaneously injected into flanks of nude mice. *n*=5 mice per group, 2 tumors per mouse, i.e. 10 tumors per shRNA treatment. **(B)** Tumor weight was determined upon dissection of euthanized animals. PLOD2-deficient tumors were slightly larger than Scr tumors (*P*=0.0495) and HIF1α-deficient tumors (*P* =0.0131). **(C)** Lungs from mice bearing KIA transplanted subcutaneous tumors. H&E staining revealed the presence of numerous metastases in control tumors (large purple areas) but very few in lungs from animals bearing PLOD2- and HIF1α-deficient tumors. **(D)** % Tumor burden was evaluated with ImagePro7 software; **(***P< 0.39)* **(E)**. Loss of HIF1α in the primary tumor significantly reduced the total number of sarcoma foci in lungs (*P* <0.0001) (left panel) calculated over multiple experiments and the average number of sarcoma foci/lung (*P* =0.0500) (middle panel). Loss of PLOD2 also significantly reduced the total number of sarcoma foci in lungs (*P* <0.0001) and the average number of sarcoma foci/lung (*P*=0.0453). HIF1α and PLOD2 depletion in primary tumors also decreased the % of lungs with sarcoma foci. (right panel) **(F)** H&E, HIF1α, Hypoxyprobe, and Lectin staining were used to characterize control KIA tumors using a 50x objective (scale bar; 200 μm) and a 200x objective (scale bar; 100 μm). Black boxes indicate enlarged areas; arrow (left panel) indicates HIF1α-positive cells. Arrow (right panel) indicates lectin-positive cells of a blood vessel. **(G)** Picrosiruis stain was used to characterize collagen organization in subcutaneous KIA tumors. Deletion of HIF1α and PLOD2 altered collagen organization. Scale bar=50 μm. **(H)** 4-12% NuPage Bis-Tris (top panel) and 3-8% Tris-Acetate (middle panel) gradient gels were used to characterize

collagen structure in KP cells treated with scr, HIF1α, or PLOD2 shRNA. *monomers, **dimers, and ***trimers of collagen I were detected. Confirmation of PLOD2 and HIF1α deletion was established using standard 10% SDS-PAGE gels (bottom panel). Hypoxia exposure lasted 16 hours. **(I)** Hydroxyproline modifications on collagen were measured using acid hydrolyzed tumor tissue. Deletion of HIF1α (P= 0.0536) and PLOD2 (P=.0102) increased hydroxyproline levels compared with scramble control.

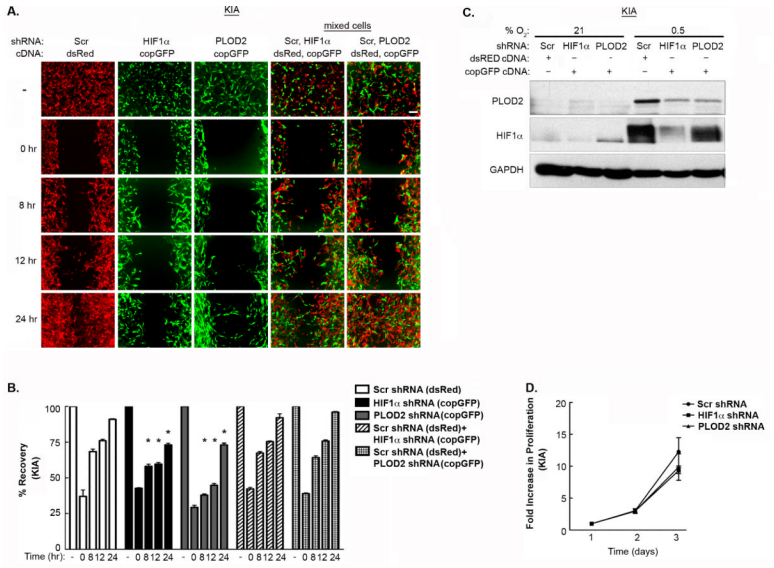

Figure 3. HIF1α and PLOD2 mediate sarcoma cell migration via a cell extrinsic mechanism

(A) Scratch migration assays of confluent, and therefore oxygen and nutrient-limited, KIA cells stably expressing Scr, HIF1α, or PLOD2 specific shRNAs and either copGFP (HIF1α, PLOD2) or dsRed (Scr). Green and Red cells were mixed 1:1. **(B)** Quanitfication of recovery in (A) (all *P* values are ≤ 0.0105). **(C)** Western blot analyses of KIA cells treated as in (A) and (B). ShRNA-mediated knockdown of HIF1α and PLOD2 shown here also reflects knockdown occurring in panels (A) and (B) as cell lines generated for these assays were then transduced with copGFP lentivirus of dsRed lentivirus. **(D)** Proliferation of KIA cells expressing Scr, HIF1α, or PLOD2 specific shRNAs under hypoxic conditions. Cells were counted daily.

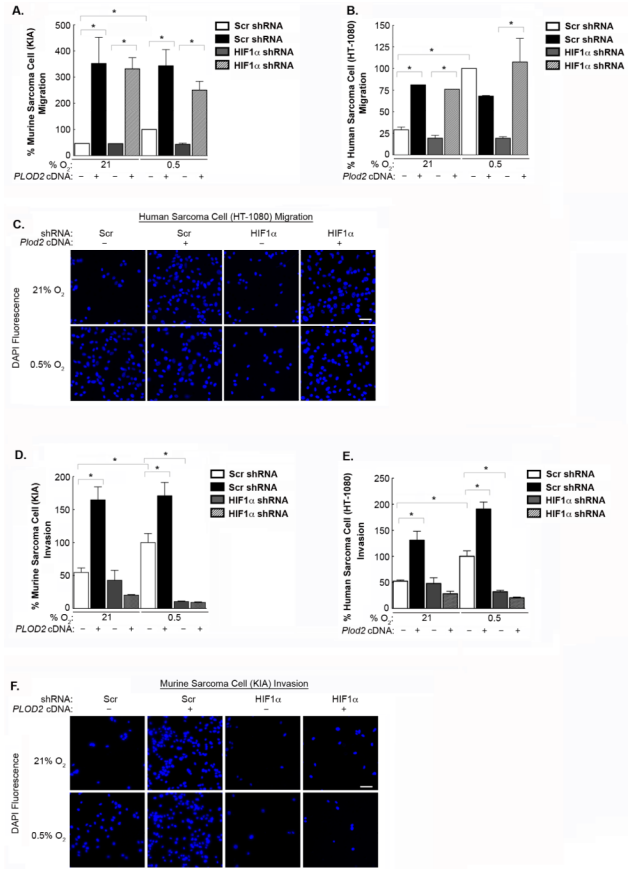

Figure 4. PLOD2 expression rescues sarcoma migration but not invasion

(A) Quantification of migration assays of normoxic and hypoxic KIA cells expressing Scr or HIF1α specific shRNAs and ectopically expressing control or wild type human *PLOD2* cDNA. All *P* values are ≤ 0.0432) **(B)** Quantification of HT-1080 migration assays performed as in (A) except murine *Plod2* was ectopically expressed. All *P* values are ≤ 0.0431. **(C)** Representative images of boyden chamber migration assay using HT-1080 cells treated as in (B). (scale bar; 50 μm). **(D)** Quantification of invasion assays of normoxic and hypoxic KIA cells expressing Scr or HIF1α specific shRNAs and ectopically expressing control or wild type human *PLOD2* cDNA using matrigel coated transwell invasion chambers. All *P* values are ≤ 0.0084. **(E)** Quantification of HT-1080 invasion assays performed as in (D) except murine *Plod2* was ectopically expressed. All *P* values are ≤ 0.0017. **(F)** Representative images of matirgel coated chamber invasion assay using KIA cells treated as in (D) (scale bar; 50 μm).

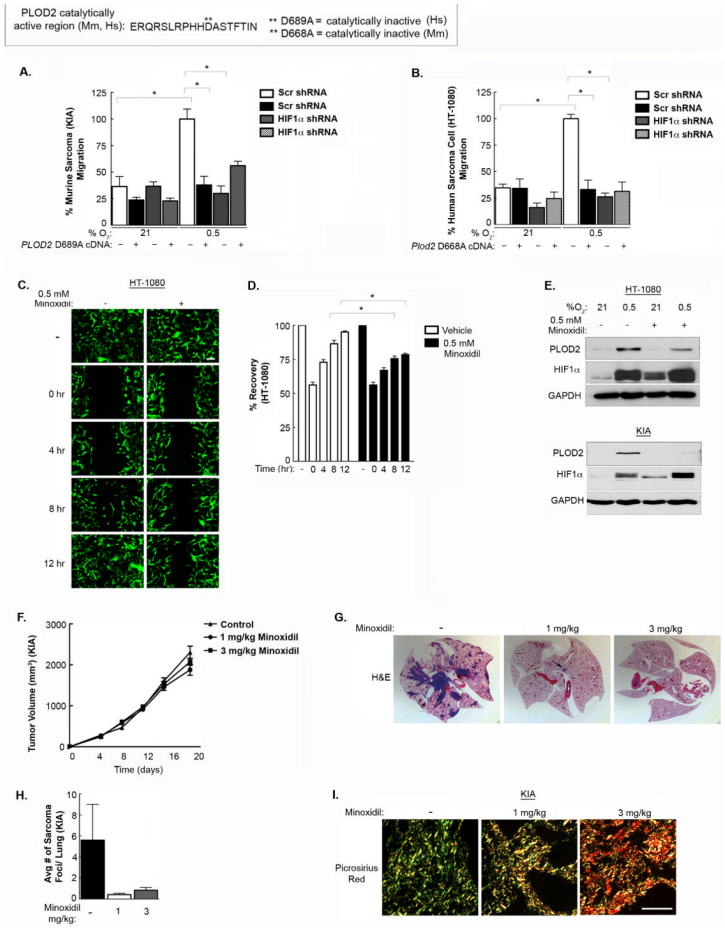

Figure 5. PLOD2 control of cell migration and metastasis is dependent upon its lysyl hydroxylase activity

(A) Quantification of migration assay of normoxic and hypoxic KIA cells expressing Scr or HIF1α specific shRNAs and ectopically expressing control or mutant human *PLOD2* D668A cDNA (all *P* values < 0.0001). **(B)** Quantification of migration assay of normoxic and hypoxic HT-1080 cells expressing Scr or HIF1α specific shRNAs and ectopically expressing control or mutant murine *Plod2* D689A cDNA (all *P* values ≤ 0.0106). **(C)** Scratch migration assays of HT-1080 cells stably expressing copGFP in the presence or absence of 0.5 mM Minoxidil pretreatment for 48 hrs. **(D)** Quantification of recovery from (C) (*P* values are ≤ 0.0058). **(E)** Western blot analyses of HT-1080 and KIA cells treated as in (C,D). **(F)** Tumor allograft growth using $1x10^6$ KIA cells subcutaneously injected into flanks of nude mice. n=10 mice per group, 2 tumors per mouse, i.e. 20 tumors per treatment with vehicle or Minoxidil. **(G)** Lungs from mice bearing KIA transplanted subcutaneous tumors treated with PBS or Minoxidil. H&E staining revealed the presence of numerous metastases in control tumors (large purple areas) but very few in lungs from animals treated with Minoxidil. **(H)** Intra-peritoneal Minoxidil treatment reduced the average number of sarcoma foci/lung. **(I)** Picrosirius red staining of KIA subcutaneous tumors from (F). Minoxidil treatment altered collagen organization in the primary tumors, (scale bar; 50 μm).

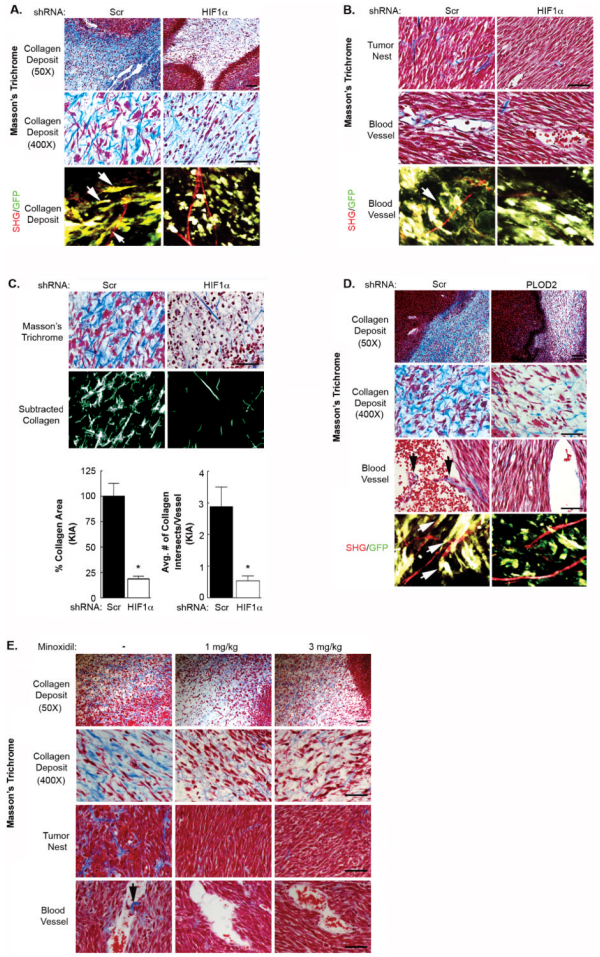

Figure 6. Sarcoma cell migration, access to vasculature, and metastasis are dependent on HIF1α/PLOD2-mediated production of disorganized collagen *in vivo*

(A) Masson's Trichrome staining and SHG of collagen in Scr and HIF1α-deficient KIA tumors. Images of various tumor areas were taken, including areas of significant collagen deposition (collagen deposit). Scale bars for 50x images represent 200 μm and scale bars for 400x images represent 50 μm. SHG: collagen (red); tumor cells (green). Arrows indicated areas where tumor cells are elongated and adhere to collagen fibers. **(B)** Masson's Trichrome staining and SHG of collagen in Scr and HIF1α-deficient KIA tumors. Images show areas lacking large amounts of collagen (tumor nest), and tumor vasculature (blood vessel). **(C)** Quantification of collagen deposition in Scr and HIF1α-deficient KIA tumors. ImagePro7software subtracted red hues from images, leaving only blue (collagen) stain to be measured. Collagen to be quantified is outlined in green, and ImagePro7 software calculated these areas P <0.0001 (lower left panel). Number of collagen intersects/blood vessel was counted manually from 12 images and 4 separate primary tumors P =0.0016. **(D)** Masson's Trichrome staining and SHG of collagen in Scr and PLOD2-deficient KIA tumors. Scale bars for 50x images represent 200 μm and scale bars for 400x images represent 50 μm. Arrows indicated areas where tumor cells are elongated and adhere to collagen fibers. **(E)** Masson's Trichrome staining of control and Minoxidil treated KIA tumors. Arrow indicates the presence of collagen and tumor cells in the vasculature. Scale bars for top row 50x images represent 200 μm and scale bars for remaining row 400x images represent 50 μm.

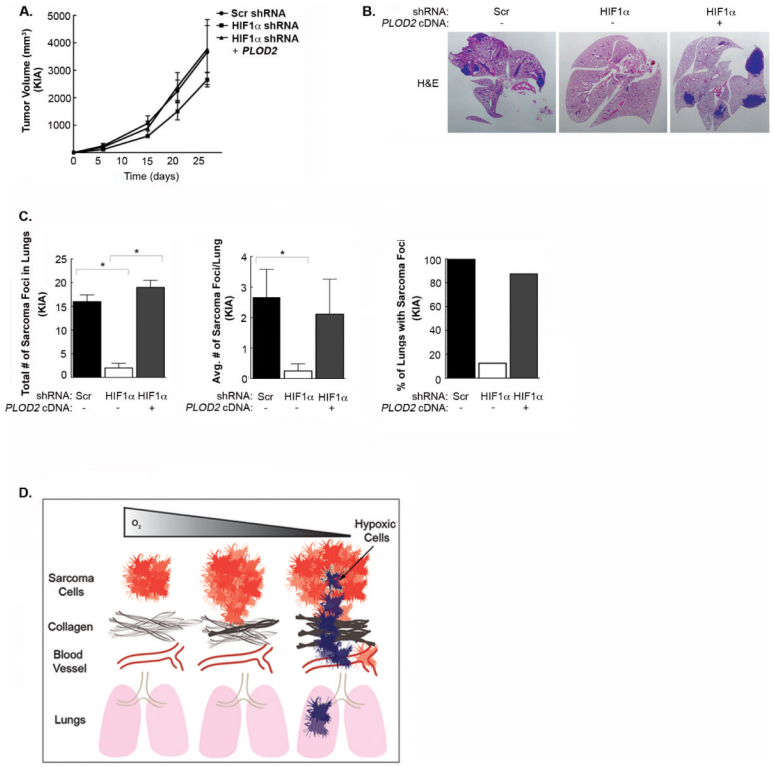

Figure 7. Expression of PLOD2 restores metastasis in animals bearing HIF1α-deficient sarcomas

(A) Tumor volume from Scr, and HIF1α-deficient, as well as HIF1α-deficient tumors that stably express the wild-type *PLOD2* expression vector (rescue) n=6 mice per group, 2 tumors per mouse; i.e. 12 tumors per shRNA treatment. **(B)** H&E staining of lungs from Scr, HIF1α-deficient, and rescue tumor groups (HIF1α shRNA+ *PLOD2).* Metastases are stained dark purple. **(C)** Quantification of lung metastases from tumors in (B). (left panel) Total number of sarcoma foci in lungs from HIF1α-deficient tumors is decreased compared to Scr (P=0.0083) and to HIF1α + *PLOD2* cDNA (P =0.0199). (middle panel) Average number of sarcoma foci/lung is decreased in HIF1α-deficient tumors P =0.0132. (right panel) % of total lungs containing sarcoma foci in all three groups. **(D)** Model of hypoxia-dependent effects on collagen and metastasis in sarcomas.